# Equilibrium shapes of a nematic–smectic-*B* liquid-crystal interface

Ágnes Buka and Tibor Tóth Katona
*KFKI, Research Institute for Solid State Physics of the Hungarian Academy of Sciences, H-1525 Budapest, P.O. Box 49, Hungary*

Lorenz Kramer
*Institute of Physics, University of Bayreuth, 95440 Bayreuth, Germany*
(Received 2 November 1993; revised manuscript received 4 February 1994)

Equilibrium shapes of the nematic–smectic-*B* liquid-crystal interface have been investigated. Three types of smectic-*B* germs with different orientation in a quasi-two-dimensional geometry have been found at small undercooling. Two of these have a similar, rectanglelike shape with two long faceted sides; the third is circular with a small hexagonal modulation. By heating the rapidly grown smectic phase the nematic phase is nucleated below the phase transition. Nematic monodomains were detected for different alignments having a nonfaceted, oval form. From the shape of the germs the angle dependence of the surface tension was determined.

PACS number(s): 61.30.−v, 61.50.Cj, 64.70.Md

## I. INTRODUCTION

Experimental investigations of equilibrium shapes of crystals are generally very difficult because of the large equilibration times, even for quite small crystallites. Thus, in metal crystallites of a few micrometer diameter at temperatures of several hundreds degrees Kelvin equilibration times of a few days were observed [1]. An exception is helium crystals in superfluid helium where transport is extremely rapid, and here the best evidence for a roughening transition has been found [2].

The solidlike liquid-crystalline phase smectic-*B* (Sm-*B*) is a good candidate for equilibrium-shape measurements, since transport is rather fast. In addition the very large anisotropies lead to interesting effects. The usual mesomorphic phase sequence on cooling is isotropic (*I*)–nematic (*N*)–Sm-*A*–Sm-*B*, possibly followed by more ordered smectics before the substance fully crystallizes [3]. However, in rare cases one has a direct *N*–Sm-*B* transition which is the subject of this paper. *N* is characterized by purely orientational order, and Sm-*B* has, in addition, layers perpendicular to the preferred molecular axis (director) with hexagonal positional order inside the layers [4]. This ordering makes the structure stiff against bending of the layers in contrast to the Sm-*A* phase, where there is no positional order inside the layers. As a consequence, at the *N*–Sm-*A* (or *I*–Sm-*A*) transition usually focal conic structure [7] or in rare cases filamentary growth is observed [8]. To describe the equilibrium shapes one has to treat bulk, surface, and elastic energies together [9].

The equilibrium shapes in the Sm-*A*–Sm-*B* and *N*–Sm-*B* transitions, on the other hand, should be described by the classical Wulff construction which gives the shape of crystallites in terms of the angle-dependent surface tension (or energy) only [10]. In fact, a measurement of an Sm-*B* germ in an Sm-*A* environment has been performed previously [11] (see also below). The less common *N*–Sm-*B* transition is particularly interesting since it is the one where rapid dendritic mesophase growth has been observed at large undercoolings [12]. In fact, a sequence of morphological transitions as a function of undercooling was observed which have not yet been explained.

Motivated by these facts, we have performed experiments on the *N*–Sm-*B* interface in a thin layer where smectic germs were grown very slowly and then kept at fixed size essentially at the transition temperature $T_{NS}$. In this way we were able to determine the equilibrium shapes of three types of Sm-*B* germs with different orientation in a quasi-two-dimensional geometry, and extract from that the angle dependence of the surface tension. Strong faceting along the planes of the Sm-*B* layers but no discontinuities in the slope (cusps) was found.

A very surprising feature occurred during the reverse process, when melting the smectic which had been grown rapidly from many dendrites. Nematic germs appeared already substantially below $T_{NS}$. Most of them had a uniform oval shape totally different from that of the smectic germs (no faceting). This provides evidence that fast dendritic growth produces a disordered, but optically homogeneous type of smectic phase.

## II. EXPERIMENTAL

Three liquid-crystalline substances were used for the experiments, each of them having a *N* to Sm-*B* first-order phase transition at $T_{NS}$,

I. 4-n-propyl-4'-cyano-trans 1,1-bicyclohexane, $T_{NS} = (56.3°C)$


 

II. 4-n-butyl-N-[4-(p-cyanophenyl)-benzylidene]-aniline, $T_{NS} = (87.4°C)$

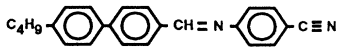


III. 4-n-propyl-4'trifluoromethoxyphenyl-ethylene-trans 1,1- bicyclohexane,

$T_{NS} = 77.0°C$

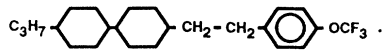


The $T_{NS}$ values of substances I and II given in parenthesis indicate a monotropic Sm-*B* transition, while III exhibits the phase on cooling and on heating from below the crystallization temperature. Substance I was investigated by x-ray scattering [13] and it was found to be an interdigitating bilayer structure with a weak three-dimensional (3D) ordering, thus, a crystalline Sm-*B*. We are not aware of similar structural analyses of substances II and III, but the fact that they do not exhibit an Sm-*A* phase makes it likely that their Sm-*B* phase is also crystalline (rather than hexatic), see, e.g., [6]. The *N*–Sm-*B* phase transition appears to be of a rather well-developed first-order type. Its latent heat ($\sim 10^4$ J/kg) is about the geometric mean of the latent heats of the *I*-*N* and the Sm-*B*–crystal transitions, these two differing by a factor of about 30. Since noticeable supercooling is possible in the absence of nucleation sites pretransitional fluctuations should be fairly small.

Cells of dimensions $10 \times 10$ mm$^2$ and of thickness $d = 10$ $\mu$m bounded by glass plates were prepared. Samples of both surface alignments of the nematic director—homeotropic and planar—were prepared, with an exception of substance III for which no homeotropic orientation could be achieved.

The sample temperature was controlled in a hot stage with an accuracy of 0.002 °C. The growth process was observed in a polarizing microscope equipped with a CCD video camera. The images were recorded and fed into a personal computer for digital analysis with spatial resolution of $512 \times 512$ and 256 gray scaling for each pixel.

## III. RESULTS AND DISCUSSION

Formation of the Sm-*B* phase was observed at and just below $T_{NS}$ (undercooling $\Delta T = T_{NS} - T$). Experiments were carried out with smectic seeds formed spontaneously below $T_{NS}$ as well as with single germs which were prepared by heating spontaneous ones back up to $T_{NS}$. The general, quantitative features of the slow growth and the equilibrium state are as follows.

The Sm-*B* phase nucleates in the nematic fluid, away from the glass plates (in the interior of the sample) which is a favorable condition for creating perfect smectic ordering. The director of the smectic body is presumably parallel with that of the nematic phase until its diameter approaches the sample thickness. During further growth the germ usually prefers an orientation where its director is parallel with the glass surfaces (smectic layers are perpendicular to them). This situation is naturally fulfilled for planar initial alignment. In the homeotropic samples most germs turn by an angle of $\pi/2$ when reaching the glass plates. We suppose, a nematiclike boundary layer exists close to the glass plates [14].

The shape of this type of planar Sm-*B* monodomain in equilibrium with its nematic phase is similar for all cases studied. Typical examples are shown in Figs. 1(a) and 1(b) for substance I. In both cases the smectic layers are perpendicular to the glass plates and parallel with the two long straight facets of the germ, while the surrounding nematic is planar in Fig. 1(a) and homeotropic in 1(b). Note the slightly convex boundaries on the short sides. This form of the interface can be stabilized for a long time (we kept germs up to 24 h) with careful temperature adjustment within a range of 0.02 °C. However, it is difficult to determine the equilibrium value $x$ of the (maximum) length to width ratio to better than about 20%. Depending on substance and alignment $x$ varies in the range of 1.5–6 which is an extremely large shape anisotropy compared to values of well-studied organic crystal-melt interfaces. (For succinonitrile, the anisotropy is 0.005 [15].) For a given liquid crystal $x$ is smaller by about 60% in the homeotropic alignment than in the planar one.

The shape anisotropy factor $x$ is equal to the ratio of $\sigma_{\parallel}/\sigma_{\perp}$, where $\sigma_{\perp}$ and $\sigma_{\parallel}$ are the values of the surface tension for interfaces perpendicular to the director in the Sm-*B* phase (along the long edge of the germ) and parallel to it, respectively. It is interesting to note that from the different values of $x$ for the homeotropic and planar alignment one can get an estimate of the order of magnitude of the surface tension of the Sm-*B*–*N* interface which has, to our knowledge, not been determined before. In the homeotropic case one has additional contributions to the surface energy coming from the elastic deformation of the nematic near the interface which is of splay-bend type along the long edges and mainly twist along the short ones. This deformation zone has a width of order of the sample thickness $d$ and appears to be barely visible, see Fig. 1(b). The elastic-energy contribution is of the form $\alpha K/d$ where $K$ is the relevant combination of elastic constants and $\alpha$ is a numerical factor. Since one has $K_{22} < K_{11}, K_{33}$, where $K_{11}$, $K_{22}$, and $K_{33}$ are the usual splay, twist, and bend elastic constants, respectively, the contribution is somewhat smaller on the short side where the surface tension is higher. Clearly, the germ in the homeotropic environment should be less anisotropic, as observed experimentally. With $x = 5$ in the planar and $x = 3$ in the homeotropic case, and a deformation energy ratio of 1.3 (which is a rough estimate of the splay-bend

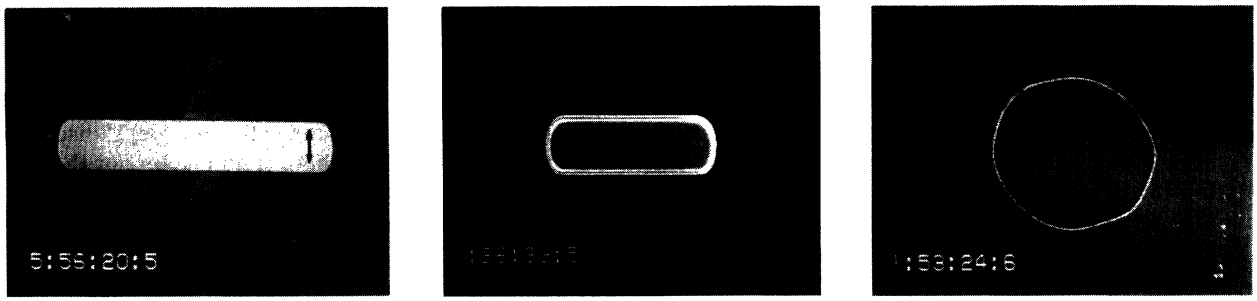


FIG. 1. Microscopic images of equilibrium shapes of Sm-$B$ germs in contact with the nematic phase, $d=10\ \mu$m, $\Delta T=0.1\,^{\circ}$C. In order to obtain the age of the Sm-$B$ monodomains 10 h has to be added to the counting given in the pictures. Double arrows indicate direction of director. (a) Planar Sm-$B$ in planar $N$ (b) Planar Sm-$B$ in homeotropic $N$ (c) Homeotropic Sm-$B$ in homeotropic $N$.

elastic contribution divided by the twist) one gets $\sigma_{\perp}=1.5\alpha K/d$, which leads to $\sigma_{\perp}=1.5\times10^{-2}$ erg/cm$^2$ for $K=10^{-6}$ dyn, $d=10\ \mu$m, and $\alpha=10$. This value is of the order of experimental values measured for nematic-isotropic interfaces [16] and one order of magnitude smaller than that obtained for an Sm-$A$–Sm-$B$ interface [11]. Possibly $K$ is considerably larger than the value we took, since elastic constants are expected to increase near the transition point to the Sm-$B$ phase. One can also compare this surface-tension value with the anchoring energy coefficient which determines the strength of the orientational surface ordering of a nematic on a solid interface. This quantity depends of course on the quality of the substrate surface, on the treatment procedure, on the material parameters of the nematic, on the temperature, etc. [17], but typically lies in the region of $10^{-3}$–$10^{-2}$ erg/cm$^2$ [18,19] and is comparable to our $\sigma_{\perp}$.

The faceting of the equilibrium germs along the smectic layers indicates that in the Sm-$B$ there is long-range order with undeformed planes. The angle-dependent surface tension $\sigma(\theta)$, where $\theta$ describes the orientation of the surface, can be extracted up to a normalization factor from the equilibrium shape by the Wulff construction [10]. In Fig. 2(a) we show $\sigma(\theta)$ normalized to $\sigma(0)=\sigma_{\parallel}$ (continuous curve) as obtained from the germ in Fig. 1(b), the boundary of which is described by $r(\varphi)$ (shaded region; the Wulff construction is indicated). The plot can be continued symmetrically into the other quadrants. The cusp of $\sigma(\theta)$ at $\pi/2$ expresses the faceting. Note that $\theta$ appears to be a continuous function of $\varphi$. Since all surface orientations occur (no "forbidden" directions) the surface stiffness $\sigma(\theta)+\sigma''(\theta)$ is positive everywhere [10].

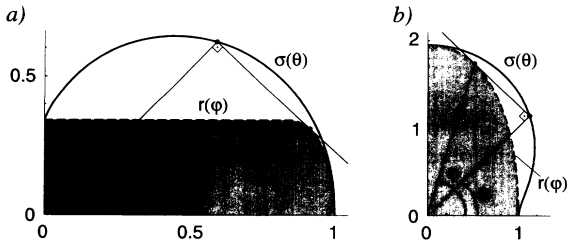


FIG. 2. Wulff plots showing the angle dependence of the surface tension $\sigma(\theta)$ for (a) Sm-$B$–$N$ and (b) $N$–Sm-$B$ interface.

This is in contrast to the measurement of an Sm-$B$ germ in an Sm-$A$ environment [11] which was found to be cusped at the short ends, so that there $\sigma''(\theta)<-\sigma(\theta)(<0)$. It is curious to note that in our case, $\sigma(\theta)$ has a minimum at $\theta=0$, so that $\sigma''(0)>0$. In fact the minimum is very shallow: $\sigma(\theta)$ increases from its value $\sigma_{\parallel}$ at $\theta=0$ by about 0.1% at $\theta\approx7^{\circ}$ and then decreases monotonically to $\sigma_{\perp}\approx\sigma(0)/3$ at $\theta=90^{\circ}$. It is an interesting question whether the qualitative different behavior of the surface tension in the two systems has some fundamental relevance.

The elongated, rectanglelike shape [Fig. 1(a), (b)] described above persists in a small range of undercooling ($\Delta T<0.3\,^{\circ}$C), where slow dynamics are observed. The growth velocity increases at the beginning, reaches a maximum, and decreases later on.

In samples with planar nematic alignment we have only found the type of germ described above, i.e., planar alignment in the smectic phase too (the same director orientation on both sides of the interface). The situation is more complex for the homeotropic samples. For substance II, there are a few among the spontaneously nucleated germs which do not turn over by $\pi/2$ when reaching the size of about the sample thickness but they stay homeotropic. In compound I, spontaneously nucleated germs always turn planar but with some effort one can induce an already existing planar germ to turn back to homeotropic alignment and to grow in this position. The procedure involves melting of a planar germ till it gets so small that it can turn back to homeotropic orientation. Then a fast cooling is applied before the germ melts and disappears completely. Due to the large undercooling the homeotropic germ grows rapidly without having a chance to turn back again. The shape it has at the very beginning of the growth is a (slightly deformed) circle, the deformation clearly indicates a hexagonal shape which reflects the symmetry of the Sm-$B$ phase in the plane of the smectic layers. This form demonstrated in Fig. 1(c) can be grown and stabilized similarly to the planar germs. The germ does not get faceted, and the hexagonal modulation developed on the circular shape is within 0.1 This structure reminds one of the results obtained for disklike molecules exhibiting a hexagonal columnar phase [20].

Concerning the rapid growth at large undercooling we want to mention that the planar germs (in both homeotropic and planar nematic surrounding) produce dendrites with four main branches [12], while the hexagonal, homeotropic ones grow a petal shape (splitting tips).

We have also studied the inverse process, namely, the formation of the nematic phase in Sm-$B$ during heating. The Sm-$B$ phase could not be overheated. At large heating rates the nematic nucleated on the glass surfaces and the melting took place at $T_{NS}$. At slow heating rates the melting scenario was strongly influenced by the thermal history of the sample. Slowly grown equilibrium smectic germs ("perfect" ordering) melt by moving the $N$–Sm-$B$ interface (they shrink) at $T \geq T_{NS}$. The rapidly grown smectic phase behaves differently: nematic germs appear far (several degrees) below $T_{NS}$ and stay in equilibrium with the Sm-$B$. The germs grow steadily in number and size with increasing temperature. The state of the system then appears to be a function of temperature only. The location of the first nematic seeds are the boundaries between slightly misaligned ($<7°$) smectic domains originating from different germs. In fact we observed that the melting temperature was lower where the misalignment was larger. If the domain boundary is roughly parallel to the director there appears a long nematic channel separating the domains. Otherwise the equilibrium shape of the nematic islands imbedded in Sm-$B$ has a rather uniform oval (nearly elliptic) form with its long axis parallel to the director of the Sm-$B$. In Fig. 3 stable nematic monodomains are shown for initially planar and homeotropic samples 0.8 °C below $T_{NS}$. The ratio of the long and short axes is slightly affected by the initial alignment and is in the range of 1.6–2.0.

The Wulff plot giving the angle-dependent normalized surface tension $\sigma(\theta)$ is shown in Fig. 2(b) for a typical nematic germ. Whereas $\sigma(\theta)$ has a pronounced minimum at $\theta=0$, the curvature $\sigma''(\theta)$ is essentially zero at $\theta=\pi/2$. The only obvious relation we can see between the two cases represented in Figs. 2(a) and 2(b) is that the difference between the (normalized) surface tensions of the nematic and the smectic germs is a nonnegative, monotonically decreasing function of $\theta$. One might interpret this in terms of a reduction of the surface tension by long-range order of the smectic planes, this reduction being larger for surfaces oriented more parallel to the planes.

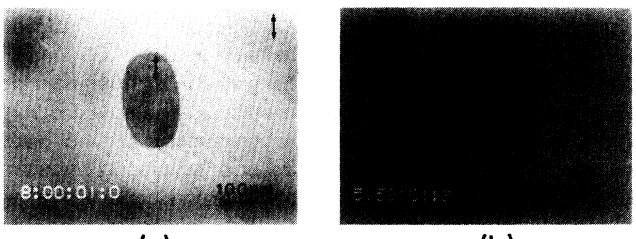


FIG. 3. Microscopic images of $N$ monodomains in Sm-$B$, $d=10$ $\mu$m, $\Delta T=0.8$ °C. (a) Planar $N$ in planar Sm-$B$ (b) Homeotropic $N$ in planar Sm-$B$.

The features described above indicate that the Sm-$B$ phase, when produced by rather rapidly growing smectic germs, is of a different nature than that produced in quasiequilibrium growth. We suggest that the rapidly grown phase has no long-range Sm-$B$ order ("disordered" smectic) and, therefore, there is no faceting of the nematic germs. Since this disordered phase is metastable having a higher free energy it must melt already below $T_{NS}$. Presumably the broad range of this transition to nematic is connected mainly with structural inhomogeneities resulting, in particular, from the domain boundaries.

In principle, the presence of impurities would also lead to broadening of the transition, i.e., two-phase coexistence over some range of temperature. However, this effect should be fully reversible, which is not the case here (the transition is essentially sharp when cooling from above, apart from the nucleation problem).

There is a rather long-range interaction between smectic germs by mutual slowing down of the growth. This can be understood from the fact that the temperature is controlled at the outer surfaces of 1-mm-thick glass plates which confine the liquid crystal. Clearly then local heat sources (germs) perturb the temperature in their neighborhood over this distance. A rather surprising effect occurred after fairly rapid heating in the presence of phase boundaries. Then there is competition of the two growth mechanisms of the nematic phase: motion of phase fronts and melting from the glass surfaces. Under these conditions the surface melting seemed to be impeded and possibly even reversed near the phase front when the front invaded a surface melted part. We doubt that this effect can be understood in terms of the heat transfer characteristics of the cell.

## IV. CONCLUDING REMARKS

We have presented an extended experimental investigation of the nucleation and slow growth of Sm-$B$ in $N$ and vice versa giving three very different types of germs in a quasi-two-dimensional sample. The fact that the hexagonal order within the Sm-$B$ layers does not lead to faceting of the homeotropic (hexagonal) germs is consistent with general principles excluding faceting in two-dimensional crystals with short-range interaction [10]. This is presumably applicable here because the correlation of the hexagonal ordering between layers is weak. By contrast, the faceting along the smectic layers in the planar germs is not excluded because the extension of the facets is in two directions much larger than molecular dimensions. Under conditions of rapid growth one apparently has kinetic roughening [12]. It would be interesting to find a way to induce an equilibrium roughening transition.

Our results for the angle dependence of the $N$–Sm-$B$ surface tension determined on the basis of the Wulff construction is presumably accurate, whereas the estimate of the absolute value is rather rough. We plan to determine the surface tension directly by measuring the contact angles between glass, Sm-$B$ and $N$ phases. This also gives some information on the wetting properties.

## ACKNOWLEDGMENT

Substance II was synthesized by K. Fodor-Csorba, materials I and III were kindly made available for us by Merck, Darmstadt. We thank H. Roeder for useful discussions. The work was financially supported by the Deutsche Forschungsgemeinschaft (SFB 213, Bayreuth), by the Hungarian Academy of Sciences (OTKA 2976), and by the Volkswagen Foundation. A.B. wishes to thank the University of Bayreuth for its hospitality and the Alexander von Humboldt Foundation for the equipment donation.

[1] J. C. Heyraud and J. J. Metoir, Surf. Sci. **128**, 334 (1983).

[2] J. E. Avron, L. S. Balfour, C. G. Kuper, J. Landau, S. G. Lipson, and L. S. Schulman, Phys. Rev. Lett. **45**, 814 (1980).

[3] It is quite common in liquid crystals that the crystallization transition exhibits a strong hysteresis. As a result, on heating the crystal melts at a temperature that may be higher than any of the liquid-crystalline phase transitions occurring on cooling ("monotropy").

[4] We are here referring to what is now often called the "crystal *B*" phase, which has a weak 3D ordering, rather than the less common "hexatic *B*" structure, see, e.g., Refs. [5] and [6].

[5] G. W. Gray and J. W. G. Goodby, *Smectic Liquid Crystals* (Leonard Hill, Glasgow, 1984), Chap. 10.

[6] G. Vertogen and W. H. de Jeu, *Thermotropic Liquid Crystals, Fundamentals* (Springer-Verlag, Berlin, 1988), Chap. 3.

[7] J. B. Fournier and G. Durand, J. Phys. II **1**, 845 (1991).

[8] S. L. Arora, P. Palffy-Muhoray, and R. A. Vora, Liq. Cryst. **5**, 133 (1989).

[9] H. Naito, M. Okuda, and Ou-Yang Zhong-can, Phys. Rev. Lett. **70**, 2912 (1993).

[10] See, e.g., M. Wortis, in *Fundamental Problems in Statistical Mechanics VI,* Proceedings of the 1984 Trondheim Summer School, edited by E. G. D. Cohen (North-Holland, Amsterdam, 1985), p. 87; H. van Beijeren and I. Nolden, in *Structure and Dynamics of Surfaces II,* edited by W. Schommers and P. van Blankenhagen (Springer-Verlag, Berlin, 1987), p. 259.

[11] P. Oswald, F. Melo, and C. Germain, J. Phys. (France) I **50**, 3527 (1989).

[12] A. Buka and N. Eber, Europhys. Lett. **21**, 477 (1993).

[13] G. J. Brownsey and A. J. Leadbetter, J. Phys. Lett. **42**, L135 (1981).

[14] M. Cagnon and G. Durand, Phys. Rev. Lett. **70**, 2742 (1993).

[15] M. Muschol, D. Liu, and H. Z. Cummins, Phys. Rev. A **46**, 1038 (1992).

[16] S. Faetti and V. Palleschi, J. Chem. Phys. **81**, 6254 (1984).

[17] B. Jerome, Mol. Cryst. Liq. Cryst. **212**, 21 (1992); G. Durand, Liq. Cryst. **14**, 159 (1993).

[18] B. Valenti, M. Grillo, G. Barbero, and T. Valabrega, Europhys. Lett. **12**, 407 (1990).

[19] M. Nobili, C. Lazzari, A. Schirone, and S. Faetti, Mol. Cryst. Liq. Cryst. **212**, 97 (1992).

[20] P. Oswald, J. Malthete, and P. Pelce, J. Phys. (Paris) **50**, 2121 (1989).

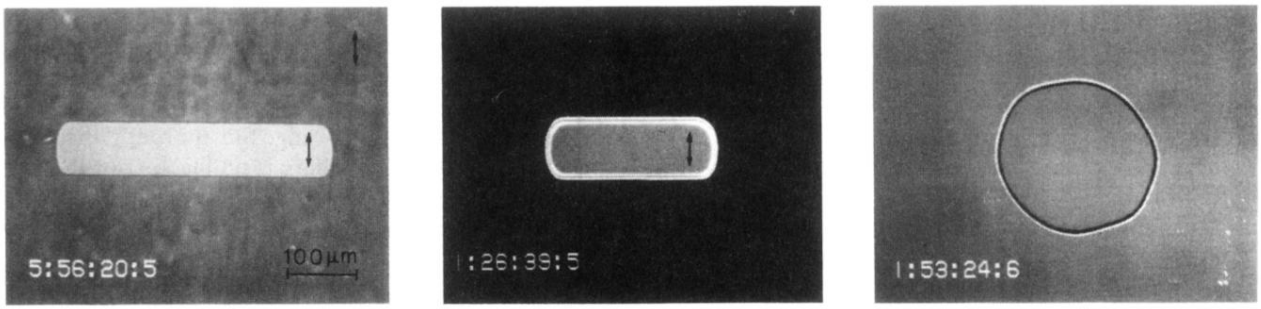


FIG. 1. Microscopic images of equilibrium shapes of Sm-*B* germs in contact with the nematic phase, $d = 10\ \mu$m, $\Delta T = 0.1\,^{\circ}$C. In order to obtain the age of the Sm-*B* monodomains 10 h has to be added to the counting given in the pictures. Double arrows indicate direction of director. (a) Planar Sm-*B* in planar *N* (b) Planar Sm-*B* in homeotropic *N* (c) Homeotropic Sm-*B* in homeotropic *N*.

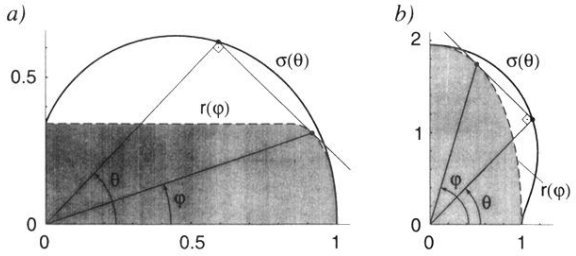


FIG. 2. Wulff plots showing the angle dependence of the surface tension $\sigma(\theta)$ for (a) Sm-$B$–$N$ and (b) $N$–Sm-$B$ interface.

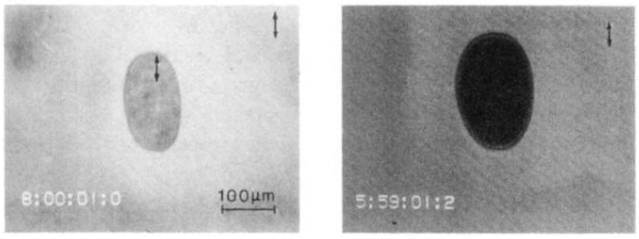


FIG. 3. Microscopic images of $N$ monodomains in Sm-$B$, $d=10$ $\mu$m, $\Delta T=0.8$ °C. (a) Planar $N$ in planar Sm-$B$ (b) Homeotropic $N$ in planar Sm-$B$.